Shape and Size Fluctuations of Microemulsion Droplets: The Role of Cosurfactant

B. Farago and D. Richter[a]
Institute Laue Langevin, 156X, 38042 Grenoble CEDEX, France

J. S. Huang, S. A. Safran, and S. T. Milner
Exxon Research and Engineering, Annandale, New Jersey 08801
(Received 8 June 1990)

Neutron spin-echo and small-angle neutron-scattering techniques were employed to study both the size and the shape fluctuations of the di-2-ethylhexyl sulfosuccinate water-in-oil microemulsion system. We observe a softening of the bending rigidity of the interface with the addition of butanol as cosurfactant. Comparison of both techniques with the theory implies that for the simultaneous description of the shape and size fluctuations both the splay and saddle-splay bending moduli are the key parameters, and the spontaneous curvature has little influence.

PACS numbers: 82.70.Kj, 61.12.Ex, 61.25.−f

It has been suggested that the properties of amphiphilic layers as they exist in microemulsions or lamellar systems are dominated by their curvature elasticity. This physical picture has been used to understand the microemulsion phase diagrams[1,2] in the bicontinuous regime. For simple droplet systems the shape fluctuations of the microemulsion globules have also been described in terms of the curvature elasticity theory.[3,4]

In this Letter we present a direct quantitative test of this theory taking into account both the predicted *static* and *dynamic* fluctuations. Employing small-angle neutron scattering (SANS), which reveals the average size distribution, and the neutron spin-echo (NSE) technique, which accesses the dynamic shape fluctuations, we find that both the splay modulus K as well as the saddle-splay modulus $\bar{K}$ must be considered to provide a consistent fit of both the statics and the dynamics. In general, the addition of cosurfactant is essential for the formation of microemulsions. We observed that butanol as cosurfactant reduces the elasticity moduli in agreement with theory.[5,6]

For our experiments we have chosen the decane-AOT-butanol-water (where AOT denotes sodium di-2-ethylhexyl sulfosuccinate) water-in-oil quaternary system because it has the advantage that the butanol content can be reduced to zero without inducing any phase transitions, and the results can be compared directly to the well-studied[7–9] ternary system.

The analysis of the experiments considers the thermal shape fluctuations of the microemulsion droplets, which distort them from their average spherical form. These fluctuations give an extra contribution to the quasielastic neutron scattering which is detected by the NSE, whereas the SANS data yield information on the time-averaged shape and on the size distribution. To optimize the information content, we used deuterated decane (which forms the oil continuum), deuterated water (the water core), and normal hydrogenated AOT and butanol (which form the film interface). The coherent-scattering-length densities of the oil and the water are nearly the same, while the AOT film has a large contrast compared to them (shell contrast). Since the scattering arises from this contrast, the detected signal comes solely from the surfactant layer, which exhibits the shape fluctuations.

The scattering form factor of a spherical shell of radius R with an infinitesimally thin wall thickness is given by $P(q) \approx [j_0(qR)]^2$, where q is the momentum transfer, and $j_0(x)$ is the zeroth-order spherical Bessel function, which has its first zero at $qR = \pi$. In reality, the polydispersity smears out this zero to a shallow minimum; nevertheless, its position accurately determines the average size and its depth contains information about the size distribution. For fitting purposes we consider the Schultz distribution[10,11] which has two parameters, the average size R_0 and a width parameter Z. The mean-square deviation is given by $\langle (R-R_0)^2 \rangle = R_0^2/(Z+1)$. For a microemulsion, Z is typically ≈ 20.

The SANS data were taken at the small-angle camera D11 of the Institute Laue Langevin (ILL) in Grenoble. We used neutrons of wavelength $\lambda = 6$ Å with a spread of $\delta\lambda/\lambda = 10\%$. The sample-to-detector distances were set at 1.25, 2.5, and 5 m. To minimize experimental errors and to make the data directly comparable, we have chosen the compositions such that the average size was roughly the same. To keep the size constant we had to choose an increasing water-AOT ratio with increasing butanol concentration (see Table I). This indicates that at least part of the alcohol is located in the interface, making more surface available; only a small fraction, if any, is in the water phase, and the rest is in the oil. Figure 1 displays the properly corrected and normalized scattering patterns for different butanol concentrations. We find that with increasing butanol concentration the minimum of the form factor becomes shallower and broader, indicating an increasing polydispersity. We further note that the intensity scattered in the forward direction also increases.

The NSE experiments were carried out at the spin-echo spectrometer IN11 at the ILL where we studied the

TABLE I. Sample composition and summary of the fitted (R_{in}, K, $\bar{K}/K$) and calculated (Z, γ, $\langle|u_2|^2\rangle$) parameters as explained in the text. The total volume fraction of AOT + D_2O + butanol in the deuterated-decane solvent was constant ($\approx 6\%$).

	D_2O/AOT (molar ratio)	Butanol/AOT (molar ratio)	R_{in} (Å)	K (kT)	$\bar{K}/K$	γ (dyn/cm)	$\langle|u_2|^2\rangle$	Z
*A*0	24.4	0	39.1	3.8	−1.89	0.07	0.011	19.7
A.5	26.3	4.5	36.9	3.0	−1.88	0.07	0.015	16.5
*A*1	28.4	9.0	32.9	2.8	−1.89	0.09	0.016	15.2
*A*3	36.6	30.1	33.1	2.0	−1.89	0.06	0.024	9.5

same samples as in the SANS experiments. We employed a neutron wavelength of $\lambda = 8.5$ Å and $\delta\lambda/\lambda = 18\%$ resulting in a time window of 0–18 ns. This allows the observation of motions which have comparable characteristic times, and detectable displacements corresponding to our wave-vector range 0.02–0.12 Å^{-1}, like the center-of-mass diffusion and, as we will show, the shape fluctuations. As explained elsewhere,[12] NSE directly measures the normalized intermeditate scattering function $I(q,t)/I(q,0)$. In the case of small fluctuations around a time-averaged spherical shell this can be written up to $o(u^2)$ as

$$I(q,t) = \left\langle \exp[-D_{tr}(R)q^2 t] V_s (\Delta\rho)^2 \left[f_0(qR) + \sum_{l\geq 2} \frac{2l+1}{4\pi} f_l(qR) \langle|u_l|^2\rangle \exp\left[-\frac{t}{\tau_l}\right] \right] \right\rangle_R , \quad (1)$$

where

$$f_0(x) = j_0(x)^2 + j_0(x) \sum_{l\geq 2} \frac{2l+1}{4\pi} \langle|u_l|^2\rangle \{[2 - x^2 + l(l+1)] j_0(x) - 2x j_1(x)\} ,$$

$$f_l(x) = [(l+2) j_l(x) - x j_{l+1}(x)]^2 ,$$

where $D_{tr}(R)$ is the tracer diffusion coefficient of the droplets, V_s is the volume of the surfactant shell, u_l is the dimensionless fluctuation amplitude of the lth mode corresponding to the lth spherical harmonics, τ_l is the corresponding relaxation time,[3,7] and $\langle\rangle_R$ stands for the average over the size distribution. This expression differs from the one in Refs. 3 and 7 by a correction term of $o(u^2)$ to the time-independent static part $[f_0(x)]$.[13] Equation (1) is model independent; the description of the dynamics enters through $\langle|u_l|^2\rangle$ and τ_l. The measured curves did not show strong deviation from a single exponential line shape. This means that in the q region where the prefactor of $\exp(-t/\tau_l)$ has a detectable amplitude in Eq. (1), $D_{tr}q^2$ and $1/\tau_l$ have comparable values. Therefore, for easy parametrization one may fit $\exp[-q^2 D_{eff}(q)t]$ to the experimental points and thereby define $D_{eff}(q)$.

We used this procedure to determine $D_{eff}(q)$ for different butanol concentrations as a function of q as shown in Fig. 2. In order to understand these NSE data we have to distinguish two q regions. At small q we average over motions on a scale of $1/q$, so up to $q \approx 1/R$ we cannot detect any internal motion or shape fluctuation. There we have $D_{eff} = D_{tr}(R)/S(q)$. From the SANS data we found that $S(q) \approx 1$ for $q > 0.03$ Å^{-1}. As is seen from Eq. (1), $I(q,t)$ is composed of a sum of exponentials with q-dependent prefactors. The peak structure of $D_{eff}(q)$ can be understood as follows: As we go from small q toward higher q, the form factor of the $l > 0$ modes starts to contribute significantly to the scattered intensity as compared to the time- and poly-

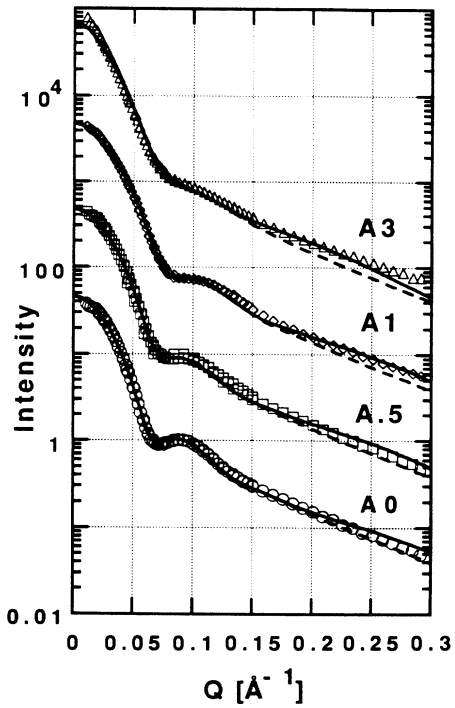

FIG. 1. SANS data for different butanol concentrations as defined in Table I. The data are shifted by a factor of 100 for better visibility. Solid lines are the result of the fit; dashed lines show what the intensity curve would be without the contribution of the form fluctuations. The error bars are smaller than the symbols. Even at the highest q the signal-to-background ratio was better than 1:2.

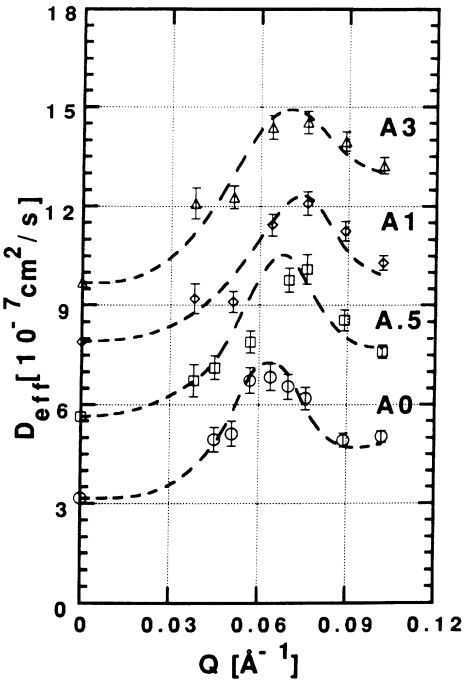

FIG. 2. NSE data as defined in the text. The dashed line is fitted to the data, represented also as D_{eff} vs q. The data are shifted by a constant 2×10^{-7} cm^2/s with respect to each other. $A0$ was not shifted. The error bars stand for $\pm1\sigma$ statistical error.

dispersity-averaged form factor ($\langle j_0(qR)^2\rangle$). This results in an increase of $D_{\text{eff}}(q)$. At $qR=\pi$, $\langle j_0(qR)^2\rangle$ reaches a minimum while the form factor of the $l=2$ mode is near its first maximum. Therefore, at this q value the relative contribution of the shape-fluctuation component reaches a maximum, and results in the observed peak. This implies, and is confirmed by the detailed fitting procedure, that this peak region is dominated by the contribution of the $l=2$ mode.

From Fig. 2 it is clear that the peak height of D_{eff} increases with the butanol content in spite of the increasing polydispersity which tends to smear out any structure. Consequently we can immediately draw the qualitative conclusion that the floppiness of the interface increases in the presence of the cosurfactant.

For the quantitative interpretation of the data we start with the theory of Milner and Safran[3] which is based on the following premise: The main restoring force for the thermal undulations of the drops is the bending energy; the total interfacial area is fixed by the quantity of surfactant in the system. The constant-surface condition is taken into account in the free energy (E) via a Lagrange multiplier γ: $E'=E-\gamma A_t$, where A_t is the total surface of the droplets to be kept constant. γ has a physical meaning; it describes the effective tension (or 2D pressure) present in the interface (this should not be confused with a macroscopic surface tension). We also include the saddle-splay energy of the Helfrich expression,[14] which comes from the Gaussian curvature:

$$E_{\text{bend}}=\frac{K}{2}\int dS\left(\frac{1}{R_1}+\frac{1}{R_2}-\frac{2}{R_s}\right)+\bar{K}\int dS\frac{1}{R_1R_2}, \quad (2)$$

where R_1 and R_2 are the two radii of curvature and R_s is the spontaneous curvature. The Gauss-Bonnet theorem implies that the saddle-splay contribution is a topological constant and in the case of droplets it gives $n4\pi\bar{K}$, where n is the number of droplets. However, with the constant-surface, constant-volume condition, varying the polydispersity varies the number of droplets; consequently $\bar{K}$ cannot be neglected. Therefore, augmenting the energy term with this expression in Refs. 3 and 4, the fluctuation amplitudes and time constants can be readily recalculated.[15] Here we are interested in the polydispersity ($l=0$ mode) and the $l=2$ modes, which dominate the NSE data. We find

$$\langle|u_0|^2\rangle=\frac{kT}{2K(6-A)},\quad \langle|u_2|^2\rangle=\frac{kT}{4KA},\quad \tau_2=\frac{\eta R^2}{KA}\frac{55}{24}, \quad (3)$$

where

$$A=4\frac{R}{R_s}-3\frac{\bar{K}}{K},$$

and

$$\gamma=\frac{K}{R_s^2}\left[6-8\frac{R}{R_s}+2\left(\frac{R}{R_s}\right)^2+3\frac{\bar{K}}{K}\right], \quad (4)$$

with η the viscosity. u_0 can be converted to the Z parameter in the Schultz distribution by $Z=(4\pi/u_0^2)-1$. The characteristic time of the size fluctuations is estimated to be in the μs range (as the water can be considered incompressible, it involves surfactant and water exchange) well out of our observation window (up to 18 ns), so this mode shows up only as a static property. Physically $\bar{K}$ couples to the number of droplets. $\bar{K}<0$ tends to favor a larger number of drops and hence increases the polydispersity (u_0). On the other hand, the $l>2$ modes make the droplet surface rippled. With the constant-total-surface constraint this decreases the number of droplets. Thus $\bar{K}<0$ tends to inhibit these modes. These trends are well reflected in Eq. (3).

At the present state we neglect any viscous dissipation which might occur in the finite thickness of the AOT interface. If it has a considerable contribution compared to the hydrodynamical dissipation, the relation between u_l and τ_l will change, essentially giving longer τ_l times. Unfortunately the present time window and accuracy of the NSE spectrometer does not allow the decomposition of the signal into multiple exponential decays [see Eq. (1)] to extract, e.g., u_2 and τ_2 separately.

A qualitative analysis of the data already allows us to draw two very important conclusions.

(1) $\bar{K}/K$ is close to -2: We know this because in the case of the decane-AOT-water system the polydispersity

is practically independent of the droplet size and is around 18%–20%.[16] In Eq. (3) we can get such a high polydispersity either by choosing K to be small or by taking A close to 6. The first solution turns out to be incompatible with the NSF data (since it gives values for u_2 which are too large), so we take $A \approx 6$. On the other hand, A should be only weakly dependent on R, which means $R_s \gg R$ and $\bar{K}/K$ must be close to -2 (see Table I). Negative $\bar{K}$ was also suggested by Binks *et al.*[17]

(2) The fit is insensitive to the spontaneous curvature R_s: It is known experimentally that the maximum droplet size is ≈ 100 Å. For $K=0$ this limit occurs at $R_{\max} \approx R_s$. When $\bar{K} \neq 0$ this limit is $R_{\max} \approx R_s(1+\bar{K}/2K)$. With the known value of $R_{\max} \approx 100$ Å and $\bar{K}/K \approx -1.9$ this gives $R_s \approx 2000$ Å. Indeed $R_s \gg R$, it has little influence on the $l=2$ mode, and the polydispersity should change rapidly only when R is close to $R_s(1+\bar{K}/2K)$.

Figure 1 shows the results of the fit with the SANS data. The dashed lines represent what the scattered intensity would be without the $L>2$ modes. In Fig. 2 $D_{\text{eff}}(q)$ was determined for the fitted points in the same way as for the measured points. Table I summarizes the final parameters. With the addition of butanol we observe a strong decrease of K with a nearly constant $\bar{K}/K$ ratio. The quantitative description gives a reduction of K from $3.8kT$ down to $2kT$ and $\bar{K}/K \approx -1.89$. We note that this negative $\bar{K}$ is absolutely essential to describe simultaneously the relatively large polydispersity and the moderate shape fluctuations. Also, in the framework of the theory[3,15] we can calculate γ, the tension present in the interface [Eq. (4); Table I]. Note that the R/R_s terms are small and $6+3\bar{K}/K$ nearly cancels as $\bar{K}/K$ is close to -2, so γ automatically becomes small.

These results differ significantly from the $K \approx 0.5kT$ reported by Borkovec and Eicke.[18] From Kerr-effect measurements they derive substantially large u_2 amplitudes and a very slow $\tau_s \approx 2.2\,\mu$s relation time. If this were true, in our observation window this mode would be invisible, which is not the case.

One of us (B.F.) acknowledges the hospitality of Exxon Research and Engineering Co. during his stay.

[a]Present address: Institut für Festkörperforschung, Forschungszentrum Jülich, PF 1913, 5710 Jülich, Germany.

[1]S. A. Safran, J. Chem. Phys. **78**, 2073 (1983); D. Andelman, M. E. Cates, D. Roux, and S. A. Safran, J. Chem. Phys. **87**, 7229 (1987).

[2]S. A. Safran and L. A. Turkevich, Phys. Rev. Lett. **50**, 1930 (1983).

[3]S. T. Milner and S. A. Safran, Phys. Rev. A **36**, 4371 (1987).

[4]M. Borkovec, J. Chem. Phys. **91**, 6268 (1989).

[5]I. Szeleifer, D. Kramer, A. Ben-Shaul, D. Roux, and W. M. Gelbart, Phys. Rev. Lett. **60**, 1966 (1988).

[6]J. Jouffroy, P. Levinson, and P. G. de Gennes, J. Phys. (Paris) **43**, 1241 (1982).

[7]J. S. Huang, S. T. Milner, B. Farago, and D. Richter, Phys. Rev. Lett. **59**, 2600 (1987).

[8]M. Kotlarchyk, S. H. Chen, J. S. Huang, and M. W. Kim, Phys. Rev. A **29**, 2054 (1984).

[9]M. Kotlarchyk, S. H. Chen, and J. S. Huang, Phys. Rev. A **28**, 508 (1983).

[10]M. Kotlarchyk, R. B. Stephens, and J. S. Huang, J. Phys. Chem. **92**, 1533 (1988).

[11]M. Kotlarchyk and S. H. Chen, J. Chem. Phys. **79**, 2461 (1983).

[12]*Neutron Spin Echo,* edited by F. Mezei, Lecture Notes in Physics Vol. 128 (Springer-Verlag, Heidelberg, 1980).

[13]The origin of this correction is that the density fluctuations have to be expanded up to $o(u^2)$ and not only to $o(u)$ in order to have all the $o(u^2)$ terms in $I(q,t)$, which is proportional to the square of the density. In the $q=0$–0.12 Å^{-1} range this contribution is less than 10% and it was neglected in Ref. 3.

[14]W. Helfrich, Z. Naturforsch. C **28**, 693 (1973).

[15]S. A. Safran (to be published).

[16]Our unpublished results.

[17]B. P. Binks, J. Meunier, O. Abillon, and D. Langevin, Langmuir **5**, 415 (1989).

[18]M. Borkovec and H.-F. Eicke, Chem. Phys. Lett. **157**, 457 (1989).